Structure, magnetism and magnetocalorics of Fe-rich $(Mn,Fe)_{1.95}P_{1-x}Si_x$ melt-spun ribbons

Ou, Z. Q.; Zhang, L.; Nguyen, Huu Dung; Caron, L.; Brück, E.

DOI
10.1016/j.jallcom.2017.03.266

Publication date
2017

Document Version
Final published version

Published in
Journal of Alloys and Compounds

Journal of Alloys and Compounds 710 (2017) 446–451

Contents lists available at ScienceDirect

Journal of Alloys and Compounds

journal homepage: http://www.elsevier.com/locate/jalcom

Structure, magnetism and magnetocalorics of Fe-rich $(Mn,Fe)_{1.95}P_{1-x}Si_x$ melt-spun ribbons

Z.Q. Ou [a, b, *], L. Zhang [b, c], N.H. Dung [b, d], L. Caron [b, e], E. Brück [b]

[a] Inner Mongolia Key Laboratory for Physics and Chemistry of Functional Materials, Inner Mongolia Normal University, Hohhot 010022, China
[b] Fundamental Aspects of Materials and Energy, Faculty of Applied Sciences, Delft University of Technology, Mekelweg 15, 2629 JB Delft, The Netherlands
[c] BASF Nederland B.V., Strijkviertel 67, 3454 PK De Meern, The Netherlands
[d] Laboratory of Electron Microscopy and Microanalysis, Advanced Institute for Science and Technology, Hanoi University of Science and Technology, 01 Dai Co Viet Street, Hanoi 10000, VietNam
[e] Max Planck Institute for Chemical Physics of Solids, Nöthnitzer Str. 40, 01187 Dresden, Germany

ARTICLE INFO

Article history:
Received 26 November 2016
Received in revised form
28 February 2017
Accepted 22 March 2017
Available online 23 March 2017

Keywords:
Magnetocaloric effects
Mn-Fe-P-Si ribbon
Thermal hysteresis
Phase transition

ABSTRACT

Single phase $Mn_{0.66}Fe_{1.29}P_{1-x}Si_x$ ($0 \le x \le 0.42$) compounds were synthesized using the melt-spinning (rapid solidification) technique. All the compounds form in the Fe_2P-type hexagonal structure, except a Co_2P-type orthorhombic structure of the Si-free $Mn_{0.66}Fe_{1.29}P$ compound. The compounds with $0.24 \le x \le 0.42$ present a FM-PM phase transition, while the compounds with lower Si content show an AFM-PM phase transition. In the $Mn_{0.66}Fe_{1.29}P_{1-x}Si_x$ compounds, T_C and ΔT_{hys} are not only Si content dependent, but also magnetic field dependent. By increasing the Si content from $x = 0.24$ to 0.42, T_C increases from 195 to 451 K and ΔT_{hys} is strongly reduced from ~61 to ~1 K. T_C increases and ΔT_{hys} decreases with increasing magnetic field, $\Delta T_C/\Delta B$ is about 4.4 K/T. $Mn_{0.66}Fe_{1.29}P_{1-x}Si_x$ compounds show large saturation magnetic moments with values up to 4.57 μ_B/f.u.. A large MCE with a small thermal hysteresis is obtained simultaneously in Fe-rich $Mn_{0.66}Fe_{1.29}P_{1-x}Si_x$ melt-spun ribbons.

1. Introduction

Magnetic refrigeration, which takes advantage of magnetocaloric effects (MCEs) of a magnetic material, has attracted most attention due to its potential for high energy efficiency and environmentally friendly cooling technology compared with the conventional vapor compression cooling technology [1–3]. The magnetic refrigeration material plays a primary role for the technology to room temperature application. Among all the magnetocaloric materials, Mn-Fe-P-Si system [4–7] is known as one of the most promising materials - effective, cheap and non-toxic.

Most of the studies focused on the Mn-rich $(Mn,Fe)_2(P,Si)$ [5,6,9,10] system and found that the extra Mn atoms enter 3*f* sites and enhances the total magnetic moment. Usually with 0.2 extra Mn content and Si content around 0.5, the compounds show giant-MCEs, small thermal hysteresis and working temperatures around room temperature. But, our recent study shows that Fe-rich $(Mn,Fe)_2(P,Si)$ compounds exhibit even larger magnetic moment than that of in Mn-rich ones. Thus, the Fe-rich $(Mn,Fe)_2(P,Si)$ compounds could be the promising magnetocaloric materials if the magnetocaloric properties, such as hysteresis and working temperature, were improved.

However, in the Mn-Fe-P-Si system there appears to be also a metallurgical issue: it is difficult to avoid the formation of impurity phases. In most cases this impurity phase is the $(Mn,Fe)_3Si$ phase [8–10]. As reported by A. Yan et al. [11] and N.T. Trung [12] that the amount of impurity phase strongly depends on the quality of the starting materials, a melted segregation may help to avoid impurity phases in the final sample. Melt-spinning combines liquid phase segregation and rapid solidification, which may result in fine grained single phase materials. In addition, melt-spinning is also a fast sample preparation technique. Thus, this technology had been employed for synthesize of the Fe-rich Mn-Fe-P-Si compound. In this report, the phase formation, structural, magnetic and magnetocaloric properties of the Fe-rich $Mn_{0.66}Fe_{1.29}P_{1-x}Si_x$ melt-spun ribbons have been investigated.

2. Experimental details

Polycrystalline Fe-rich $(Mn,Fe)_{1.95}(P,Si)$ melt-spun ribbons were prepared using the melt-spinning technique. Appropriate

* Corresponding author. Inner Mongolia Key Laboratory for Physics and Chemistry of Functional Materials, Inner Mongolia Normal University, Hohhot 010022, China.
E-mail address: ouzhiqiang_nsd@hotmail.com (Z.Q. Ou).

http://dx.doi.org/10.1016/j.jallcom.2017.03.266
0925-8388/

proportions of starting materials, pure Mn chips (purity 99.99%), Fe granules (purity 99.98%), Si pieces (purity 99.99%) and the binary compounds $Fe_{1.21}P$ (purity 97%), were put in a quartz crucible and melted by radio frequency induction heating in an argon atmosphere. The obtained ingots were then put into a quartz tube with a nozzle at the bottom, melted and ejected through the nozzle on to the copper wheel rotating at a surface speed of 40 m/s. The as-spun ribbons were annealed at 1100 °C for 2 h before quenching into water. A total of 11 compositions (nominal) of $Mn_{0.66}Fe_{1.29}P_{1-x}Si_x$ were studied, with $x = 0$, 0.12, 0.18, 0.24, 0.30, 0.33, 0.34, 0.36, 0.37, 0.40 and 0.42. For comparison, a $Mn_{0.65}Fe_{1.30}P_{2/3}Si_{1/3}$ bulk sample was also prepared. The sample synthesis details refer to our previous work [5].

The X-ray diffraction patterns were collected at various temperatures with a PANalytical X-pert Pro diffractometer using Cu Kα radiation, a secondary-beam flat-crystal monochromator and a multichannel X'celerator detector. A superconducting quantum interference device (SQUID) magnetometer (Quantum Design MPMS 5XL) with the reciprocating sample option (RSO) mode was employed for magnetic measurements in the temperature range of 5 - 400 K and in magnetic fields up to 5 T. Measurements are performed on $1-2$ mg of powder samples and temperature scans are performed at a sweep rate of 2 K/min. The differential scanning calorimetry (DSC) measurements were carried out using a TA-Q2000 DSC instrument in the temperature range from 90 to 820 K.

3. Results and discussion

The room-temperature X-ray diffraction patterns indicate that all Si containing quaternary samples studied crystallize in the hexagonal Fe_2P-type structure (space group *P*-62*m*). Only the ternary sample $Mn_{0.66}Fe_{1.29}P$ crystallizes in the orthorhombic Co_2P-type structure (space group *Pnma*), in good agreement with earlier result [13]. While as for the generic one system $MnFeP_{1-x}As_x$, the orthorhombic Co_2P-type structure was observed for low As content with $0 \leq x \leq 0.15$ [14,15]. X-ray diffraction patterns are frequently used to determine the amount of impurity phases. In the Mn-Fe-P-Si system this is not straightforward, because the strongest characteristic reflection of the cubic $(Mn,Fe)_3Si$ phase, a well-known impurity phase of Mn-Fe-P-Si compounds, usually overlaps with the (210) peak of the main phase in the ferromagnetic state [16,17]. This implies that X-ray patterns below and above T_C need to be analyzed. As indicated by the dashed lines in Fig. 1, no $(Mn,Fe)_3Si$ impurity phase is detected. A case for determination of $(Mn,Fe)_3Si$ impurity phase by temperature dependence X-ray diffraction is shown as supplementary material [18].

Fig. 1 depicts the evolution of X-ray diffraction patterns with temperature in the 2θ range of $30° - 60°$ for the $x = 0.34$ sample in the temperature range of $298 - 488$ K recorded upon heating. Within this temperature range the $x = 0.34$ sample undergoes a ferromagnetic (FM) - paramagnetic (PM) phase transition without change in the crystal structure. The X-ray pattern at 348 K shows the coexistence of both the FM and PM phase, a characteristic feature of a first-order phase transition. With increasing temperature the (300) and (002) peaks shift towards each other, indicating the lattice constants *a* and *c* change in opposite sense.

Fig. 2 shows the temperature dependence of the lattice parameters for the $Mn_{0.66}Fe_{1.29}P_{1-x}Si_x$ compounds with $x = 0.33$, 0.37, 0.40 and 0.42. For all these compositions, the thermal evolution of the lattice parameters *c* resembles an S-shape rather than a linear response. An inverted S-shape is observed for the lattice parameter *a*. Thus, while the *c* parameter shows the expected increase with increasing temperature the *a* parameter shows a contraction upon heating over a wide range of temperatures. F. Guillou et al. [19] studied the evolution of the electrical resistivity and the Vikers micro-hardness (HV) of MnFe,(P,Si,B) compounds by thermal cycling them across the first-order transition, and correlated the size of the lattice discontinuities and the increase in defect concentration, which weakens the mechanical stability of material. Note that, with increasing Si content, the discontinuous change in lattice parameter at T_C becomes less pronounced, which may lead to an improvement of mechanical stability. Besides, T_C shifted to higher temperature with increasing Si content. Finally, the lattice parameter *a* increases while *c* decreases with increasing Si content.

These observations strongly support an exceptional coupling between the magnetism and the elastic properties of the lattice in these compounds. Obviously, this is not limited to the direct vicinity of T_C, but a rather broad temperature range above and below T_C is affected by this coupling. The width of this temperature range of this anomalous behavior appears to be inversely correlated with the size of the discontinuous change in lattice parameter at T_C. In other words, the transition is smeared out over a larger temperature interval with increasing Si content, while the nature of the transition retains first-order.

Discontinuous changes and nonlinear variations in lattice constants at and around the FM-PM phase transition, confirm the presence of a first-order magneto-elastic transition (FOMET). The coexistence of two phases at the transition is confirmed, as two sets of lattice parameters are obtained. It is interesting to note that, although the changes in lattice parameters *a* and *c* at the phase transition are of the order of a percent, as they are in the opposite sense, they result in a rather small volume change (< 0.1%), as depicted in Fig. 3. The overall thermal volume expansion is linear and the coefficient of volume expansion is 3.7×10^{-5} K^{-1}, in the same order of magnitude as pure Fe and Ni.

The temperature dependence of the magnetization of the $Mn_{0.66}Fe_{1.29}P_{1-x}Si_x$ compounds with $0 \leq x \leq 0.36$ measured in an applied magnetic field of 1 T is plotted in Fig. 4. For comparison, M-T curve of $Mn_{0.65}Fe_{1.30}P_{2/3}Si_{1/3}$ bulk sample is also plotted. For the compounds with $x = 0$, 0.12 and 0.18, an antiferromagnetic (AFM) - paramagnetic phase transition is observed, the Néel temperatures (T_N) are 208, 138 and 134 K, respectively. Note that, for the generic one system $(Mn,Fe)_{1.95}(P,Ge)$, 0.12 of Ge content triggers antiferromagnetic behavior [20]. Furthermore, in Mn,Fe(P,X) (X = As,Ge,Si) system, it is unexceptionally observed that T_C increases with increasing X content, indicating an enhancement of

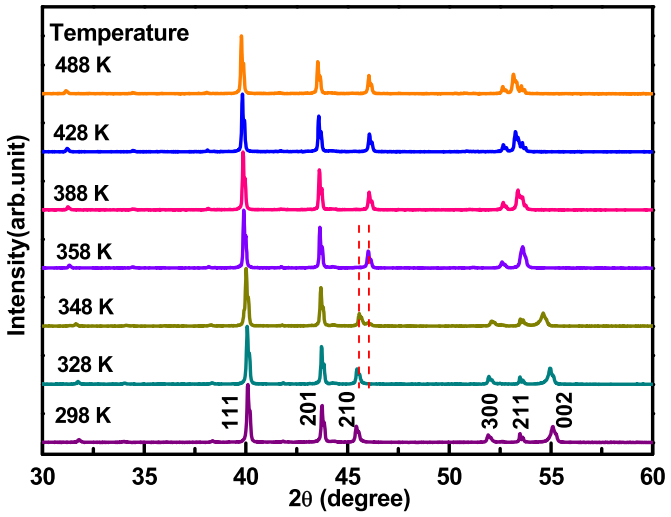

Fig. 1. X-ray diffraction patterns of $Mn_{0.66}Fe_{1.29}P_{0.66}Si_{0.34}$ recorded at different temperatures. The lines indicate the (210) peak positions before and after the phase transition.

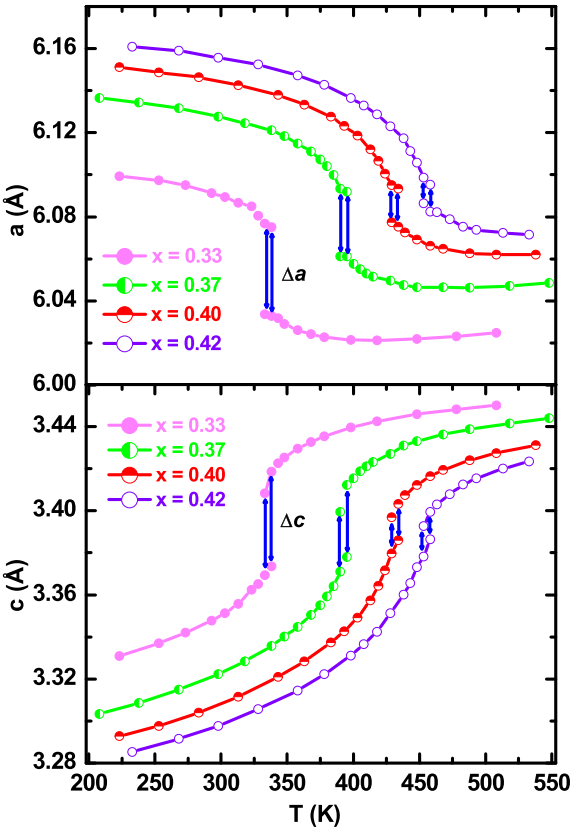

Fig. 2. Temperature dependence of the lattice parameters *a* and *c* of the $Mn_{0.66}Fe_{1.29}P_{1-x}Si_x$ compounds with $x = 0.33$, 0.37, 0.40 and 0.42 derived from X-ray diffraction patterns measured upon heating. (arrows indicate the jump in lattice parameter in the two-phase coexistence region).

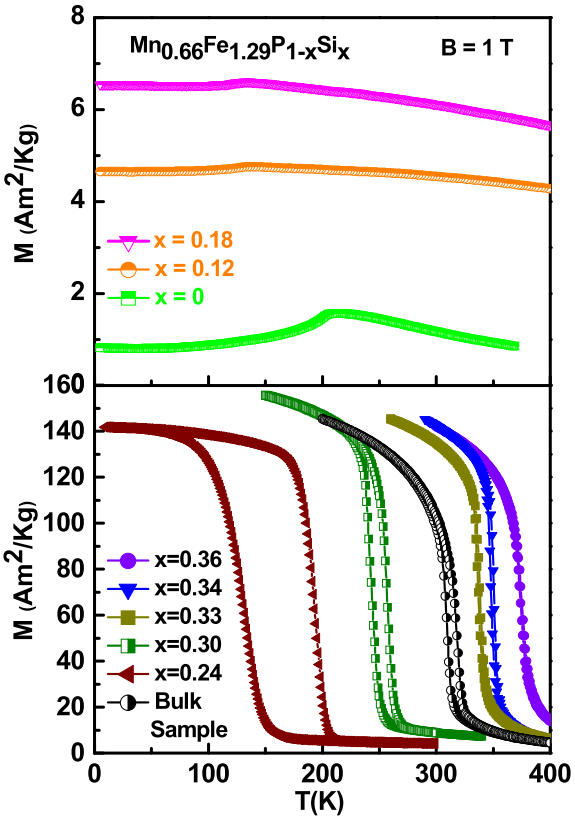

Fig. 4. Temperature dependence of the magnetization of the $Mn_{0.66}Fe_{1.29}P_{1x}Si_x$ ribbons and $Mn_{0.65}Fe_{1.30}P_{2/3}Si_{1/3}$ bulk sample measured in a field of 1 T. For the compounds with with $x = 0$, 0.12 and 0.18, measurements were performed upon cooling; for the compounds with $x = 0.24$, 0.30, 0.33, 0.34 and 0.36, measurements were performed upon both cooling and heating.

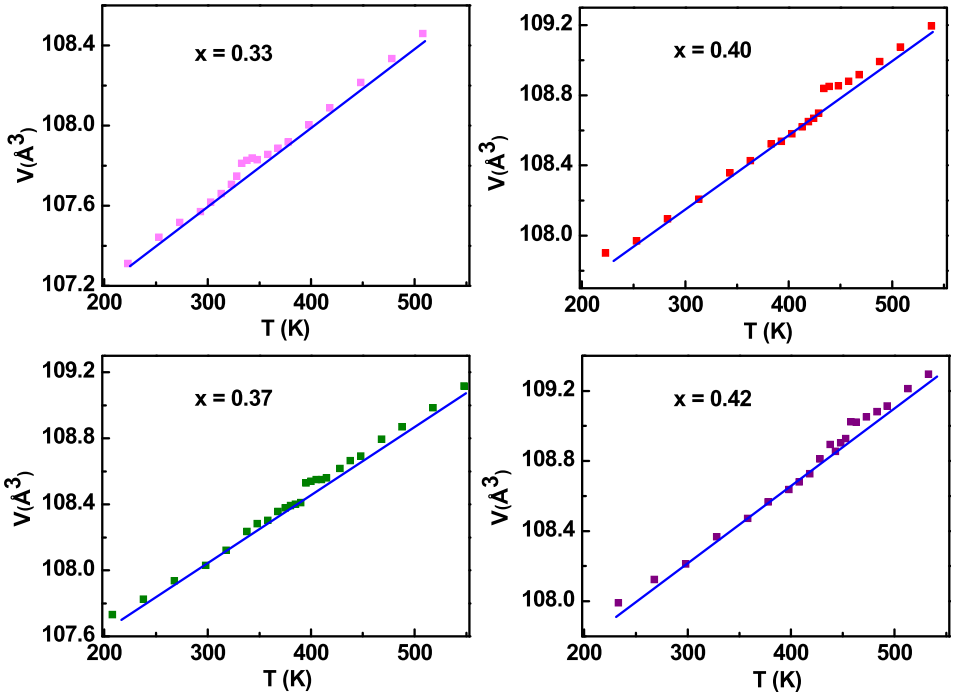

Fig. 3. Temperature dependence of the volume of the $Mn_{0.66}Fe_{1.29}P_{1-x}Si_x$ compounds with $x = 0.33$, 0.37, 0.40 and 0.42 derived from X-ray diffraction patterns measured in nitrogen atmospheres upon heating.

Table 1
Structural and magnetization data for $Mn_{0.66}Fe_{1.29}P_{1-x}Si_x$ ribbons and $Mn_{0.65}Fe_{1.30}P_{2/3}Si_{1/3}$ bulk sample.

x	Struc.	Type of the magnetic transition	T_N (K)	T_C (K)	M_s (μ_B)	ΔT_{hys} (K)	$-\Delta S_M$ (J/kgK) $\Delta B = 2$ T	Density[b] (g cm^{-3})
0	O	AFM-PM	208					
0.12	H	AFM-PM	138					
0.18	H	AFM-PM	134					
0.24	H	FM-PM		195	3.97	61	12	6.55
0.30	H	FM-PM		258	4.27	14	15	6.51
0.33	H	FM-PM		338	4.38	2	10	6.48
0.34	H	FM-PM		350	4.57	3	11	6.49
0.36	H	FM-PM		375	4.42	1	12	6.48
0.37	H	FM-PM		392[a]	4.47	2[a]		6.47
0.40	H	FM-PM		427[a]	4.43	2[a]		6.46
0.42	H	FM-PM		451[a]	3.86	1[a]		6.45
Bulk[c] sample	H	FM-PM		327	4.00	11	6	6.41

M_s is saturation magnetic moment given in μ_B/f.u., H = hexagonal, O = orthorhombic, AFM = antiferromagnetic, PM = paramagnetic, FM = ferromagnetic, the T_C values are determined from the heating M *vs.* T curves, the thermal hysteresis is measured at 1 T.
[a] The values are obtained from zero-field DSC measurements with sweeping rate of 20 K/min.
[b] The density is estimated from X-ray diffraction pattern measured at room temperature.
[c] The formula of the bulk sample is $Mn_{0.65}Fe_{1.30}P_{2/3}Si_{1/3}$.

ferromagnetic interaction of the system. For the compounds with higher Si content, a FM-PM phase transition is observed and the T_C increases from 195 K for $x = 0.24$ to 375 K for $x = 0.36$, as shown in Table 1. All the magnetization curves plotted were chosen from the second cooling-heating cycle. The so called "virgin-effect" [21,22] curves are excluded and all the magnetization curves are reproducible in subsequent cycles. For the compounds with $x \geq 0.37$, the T_C values are not measurable using the SQUID magnetometer due to the limitation of the accessible temperature range. The thermal hysteresis (ΔT_{hys}) between the cooling and heating transitions drastically reduces from ~61 K for $x = 0.24$ to ~2 K for $x = 0.33$ and the small thermal hysteresis is retained when further increasing Si content upto 42 wt% (see Figs. 4 and 5). The existence of ΔT_{hys} confirms the first-order nature of the transition, which is usually associated with the large MCE [23].

Fig. 5 shows the temperature dependence of the specific heat (C_p) for the $Mn_{0.66}Fe_{1.29}P_{1-x}Si_x$ compounds with $x = 0.37$, 0.40 and 0.42 measured in zero-field using a Differential Scanning Calorimeter (DSC). A small thermal hysteresis between the cooling (dashed lines) and heating (solid lines) is observed. The T_Cs, determined from the peak position upon heating, are 392, 427 and 451 K for $x = 0.37$, 0.40 and 0.42, respectively. The pronounced thermal effects confirm the first-order nature of the transitions.

Fig. 6 shows the magnetic field dependence of the magnetization of the $Mn_{0.66}Fe_{1.29}P_{1-x}Si_x$ compounds with $x = 0$, 0.12, 0.18, 0.24, 0.30, 0.33, 0.34, 0.36, 0.37, 0.40 and 0.42 at 5 K. For comparison, M-B curve of $Mn_{0.65}Fe_{1.30}P_{2/3}Si_{1/3}$ bulk sample is also plotted. The compounds with a Si content from 0.24 to 0.42 are ferromagnetic and their saturation magnetic moments (M_s) are between 3.86 and 4.57 μ_B/f.u.. These values are in agreement with those obtained from our neutron diffraction results [24]. Note that, the M_s values of Fe-rich $Mn_{0.66}Fe_{1.29}P_{1x}Si_x$ compounds are the largest among all the Fe_2P-based Mn,Fe(P,X) (X = As, Ge and Si) compounds [8,10,22–26].

Fig. 7 (a) shows the isothermal magnetization loops measured in the vicinity of T_C for the sample with $x = 0.33$. A pronounced magnetic field-induced PM-FM transition is observed, which is accompanied by a small magnetic field hysteresis between the field increasing and decreasing magnetization curves. These results imply the first-order nature of the magnetic phase transition. For the samples with a large thermal hysteresis, the isothermal magnetization curves were measured following the method discussed by Caron et al. [27]. The isothermal magnetic entropy change ($-\Delta S_m$) has been derived from the magnetic isotherms using

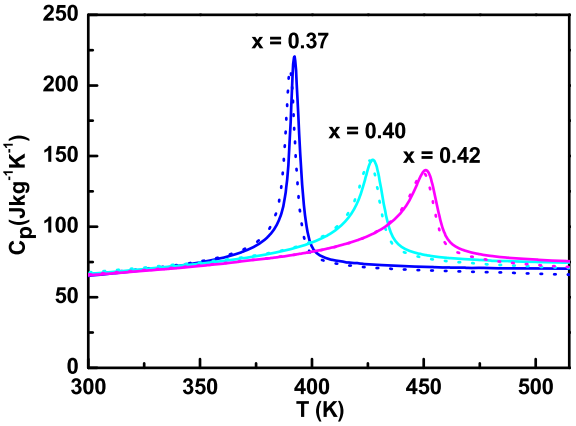

Fig. 5. Temperature dependence of the specific heat of the $Mn_{0.66}Fe_{1.29}P_{1-x}Si_x$ compounds with x = 0.37, 0.40 and 0.42 measured in zero-field upon cooling (dashed lines) and heating (solid lines).

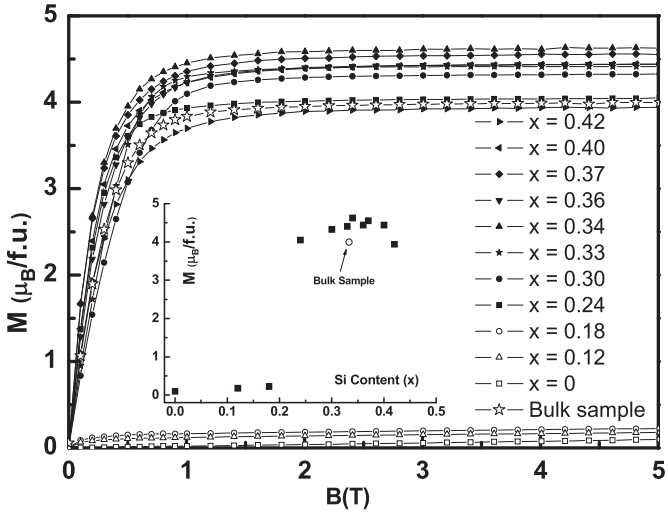

Fig. 6. Field dependence of the magnetization of the $Mn_{0.65}Fe_{1.30}P_{2/3}Si_{1/3}$ bulk sample and $Mn_{0.66}Fe_{1.29}P_{1-x}Si_x$ ribbons measured at 5 K. The insert shows the Si content dependence of maximum magnetization at 5 T.

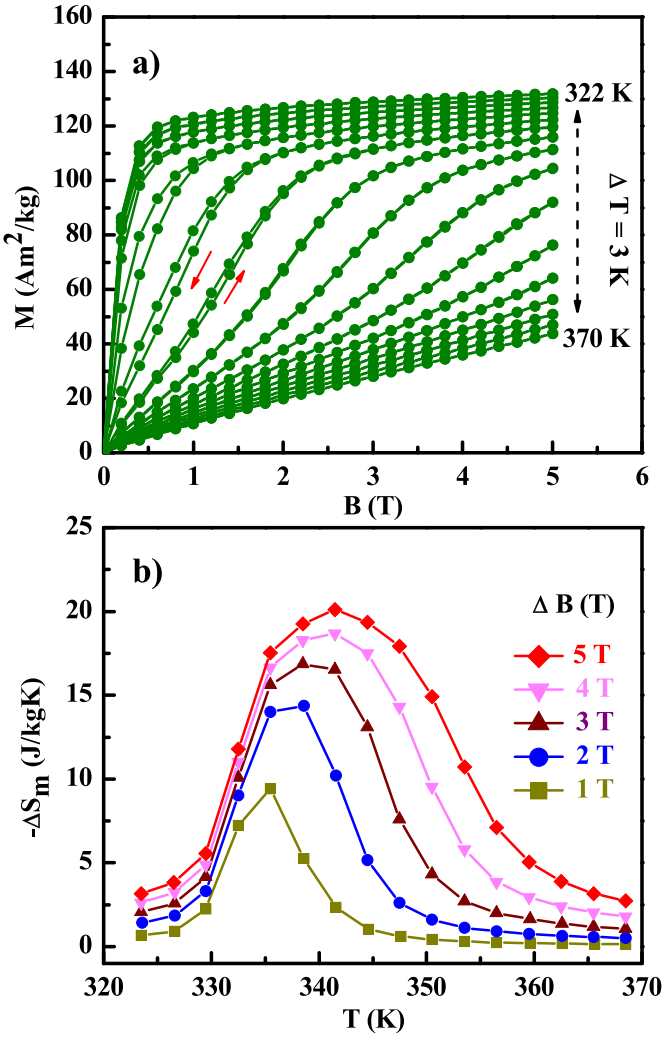

Fig. 7. Magnetic isotherms of the $Mn_{0.66}Fe_{1.29}P_{0.67}Si_{0.33}$ compound in the vicinity of its T_C (a) and the magnetic entropy changes for different magnetic field changes (b).

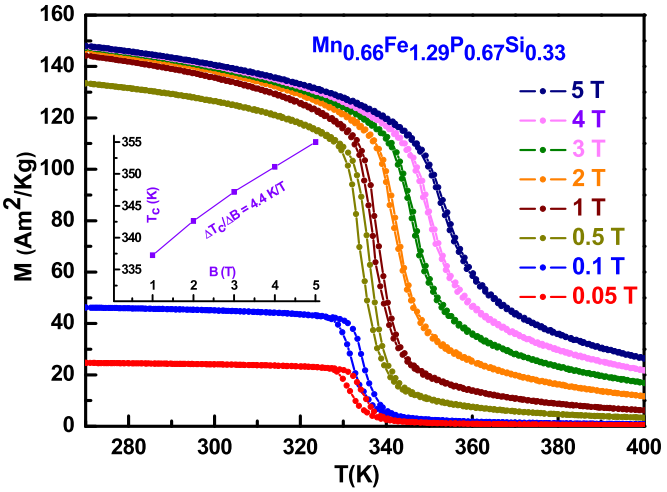

Fig. 8. Temperature dependence of the magnetization of the $Mn_{0.66}Fe_{1.29}P_{0.67}Si_{0.33}$ compound measured with increasing temperature and then decreasing temperature.

the Maxwell Equation [23]. Fig. 7 (b) shows the temperature dependence of the isothermal magnetic entropy change of the $x = 0.33$ sample in different magnetic field changes. The $-\Delta S_m$ values for $Mn_{0.65}Fe_{1.30}P_{2/3}Si_{1/3}$ bulk sample and ribbons with $x = 0.24$, 0.30, 0.34, 0.36 and 0.37 are listed in Table 1.

Fig. 8 shows the temperature dependence of the magnetization curves $M(T)$ in different magnetic fields upon cooling and heating. Both T_C and thermal hysteresis are field dependent. The T_C values on heating shift to a higher temperature with increasing field, indicating enhanced ferromagnetic interactions. The magnetic field induced PM-FM transition observed in Fig. 7 (a), is triggered by this enhanced FM interaction. The insert in Fig. 8 shows a linear increase of T_C with applied magnetic field. The rate ($\Delta T_C/\Delta B$) is about 4.4 K/T. This rate is smaller than that for $MnFeP_{0.45}As_{0.55}$ (5.2 K/T), larger than that for $Mn_{1.20}Fe_{0.80}P_{0.73}Ge_{0.25}$ (3.9 K/T) and $Mn_{1.25}Fe_{0.70}P_{0.49}Si_{0.51}$ (3.6 K/T) [7], thus we would expect a comparable value of ΔT_{ad} of our ribbons. ΔT_{hys} shows a slight reduction for increasing magnetic field.

4. Conclusions

The $Mn_{0.66}Fe_{1.29}P_{1-x}Si_x$ ($0 \le x \le 0.42$) compounds with single phase have been synthesized using the melt-spinning (rapid solidification) technique. The phase formation, crystal, magnetic and magnetocaloric properties of $Mn_{0.66}Fe_{1.29}P_{1-x}Si_x$ ($0 \le x \le 0.42$) compounds were systematically studied. All the compounds form in the Fe_2P-type hexagonal structure, except a Co_2P-type orthorhombic structure of the Si-free $Mn_{0.66}Fe_{1.29}P$ compound. The compounds with $0.24 \le x \le 0.42$ present a FM-PM phase transition, while the compounds with lower Si content show an AFM-PM phase transition.

In the $Mn_{0.66}Fe_{1.29}P_{1-x}Si_x$ compounds, T_C and ΔT_{hys} are not only Si content dependent, but also magnetic field dependent. By increasing the Si content from $x = 0.24$ to 0.42, T_C increases from 195 to 451 K and ΔT_{hys} is strongly reduced from ~61 to ~1 K, which could be correlated with the trends of discontinuous changes of lattice parameters. T_C increases and ΔT_{hys} decreases with increasing magnetic field, $\Delta T_C/\Delta B$ is about 4.4 K/T. $Mn_{0.66}Fe_{1.29}P_{1-x}Si_x$ compounds show large spontaneous magnetic moments with values up to 4.57 μ_B/f.u.. A large MCE with a small thermal hysteresis is obtained simultaneously in Fe-rich $Mn_{0.66}Fe_{1.29}P_{1-x}Si_x$ melt-spun ribbons. The compounds with a high working temperature may also be useful for other applications, *e.g.* thermomagnetic generators and heat pumps.

Acknowledgements

The authors would like to thank Anton J. E. Lefering, Michel P. Steenvoorden, and Bert Zwart (Delft University of Technology) for their help in magnetic and structural measurements and sample preparation. This work is part of the Industrial Partnership Program of the Dutch Foundation for Fundamental Research on Matter (FOM), financially supported by BASF New Business, the National Natural Science Foundation of China (Grant No. 11404176 and 51461035) and the Natural Science Foundation of Inner Mongolia of China (Grant No. 2014BS0108).

Appendix A. Supplementary data

Supplementary data related to this article can be found at http://dx.doi.org/10.1016/j.jallcom.2017.03.266.

References

[1] K.A. Gschneidner, V.K. Pecharsky, A.O. Tsokol, Rep. Prog. Phys. 68 (2005) 1479.
[2] O. Tegus, E. Brück, K.H.J. Buschow, F.R. de Boer, Nature 415 (2002) 150–152.
[3] K.G. Sandeman, Scr. Mater. 67 (2012) 566–571.

[4] O. Gutfleisch, M.A. Willard, E. Brück, C.H. Chen, S.G. Sankar, J.P. Liu, Adv. Mater. 23 (2011) 821–842.
[5] N.H. Dung, Z.Q. Ou, L. Caron, L. Zhang, D.T. Cam Thanh, G.A. de Wijs, R.A. de Groot, K.H.J. Buschow, E. Brück, Adv. Energy Mater. 1 (2011) 1215–1219.
[6] F. Guillou, G. Porcari, H. Yibole, N.H. van Dijk, E. Brück, Adv. Mater. 26 (2014) 2671–2675.
[7] H. Yibole, F. Guillou, L. Zhang, N. van Dijk, E. Brück, J. Phys. D. Appl. Phys. 47 (2014) 075002.
[8] D.T. Cam Thanh, E. Brück, N.T. Trung, J.C.P. Klaasse, K.H.J. Buschow, Z.Q. Ou, O. Tegus, L. Caron, J. Appl. Phys. 103 (2008) 07B318.
[9] N.H. Dung, L. Zhang, Z.Q. Ou, E. Brück, Appl. Phys. Lett. 99 (2011) 092511.
[10] N.H. Dung, L. Zhang, Z.Q. Ou, L. Zhao, L. van Eijck, A.M. Mulders, M. Avdeev, E. Suard, N.H. van Dijk, E. Brück, Phys. Rev. B 86 (2012) 045134.
[11] A. Yan, K.H. Müller, L. Schultz, O. Gutfleisch, J. Appl. Phys. 99 (2006) 08K903.
[12] N.T. Trung, First-order Phase Transitions and Giant Magnetocaloric Effect, PhD thesi, Universiteit van Amsterdam, The Netherlands, 2010 (Chapter 4).
[13] R. Fruchart, A. Roger, J.P. Sendteur, J. Appl. Phys. 40 (1969) 1250–1257.
[14] R. Zach, M. Guillot, R. Fruchart, J. Magn. Magn. Mater. 89 (1990) 221.
[15] M. Bacmann, J.L. Soubeyrousx, R. Barrett, O. Fruchart, R. Zach, S. Niziol, R. Fruchart, J. Magn. Magn. Mater. 134 (1994) 59.
[16] L. Zhang, E. Brück, O. Tegus, K.H.J. Buschow, F.R. de Boer, Phys. B Condens. Mat. 328 (2003) 295–301.
[17] D.T. Cam Thanh, Magnetocalorics and Magnetism in MnFe(P,Ge,Si) Materials, PhD thesis, Universiteit van Amsterdam, 2009, pp. 27–88 (Chapter 4 and 5).
[18] See supplementary material at: http://dx.doi.org/10.1016/j.jallcom.2017.03.266 for determination of $(Mn,Fe)_3Si$ impurity phase by temperature dependence X-ray diffraction.
[19] F. Guillou, H. Yibole, N.H. van DijK, L. Zhang, V. Hardy, E. Brück, J. Alloys Compd. 617 (2014) 569–574.
[20] J.V. Letao, M. van der Haar, A. Lefering, E. Brück, J. Magn. Magn. Mater. 344 (2013) 49–54.
[21] L. Zhang, O. Može, K. Prokešc, O. Tegus, E. Brück, J. Magn. Magn. Mater. 290 (2005) 679–681.
[22] Z.Q. Ou, G.F. Wang, S. Lin, O. Tegus, E. Brück, K.H.J. Buschow, J. Phys. Condens. Mat. 18 (2006) 11577–11584.
[23] A.M. Tishin, Y.I. Spichkin, The Magnetocaloric Effect and its Application, Insitute of Physics Publishing, Bristol, 2003.
[24] Z.Q. Ou, L. Zhang, N.H. Dung, L. van Eijck, A.M. Mulders, M. Avdeev, N.H. van Dijk, E. Brück, J. Magn. Magn. Mater. 340 (2013) 80–85.
[25] E. Brück, O. Tegus, X.W. Li, F.R. de Boer, K.H.J. Buschow, Phys. B Condens. Mat. 327 (2003) 431–437.
[26] M. Bacmann, J.L. Soubeyroux, R. Barrett, D. Fruchart, R. Zach, S. Niziol, R. Fruchart, J. Magn. Magn. Mater. 134 (1994) 59–67.
[27] L. Caron, Z.Q. Ou, T.T. Nguyen, D.T. Cam Thanh, O. Tegus, E. Brück, J. Magn. Magn. Mater. 321 (2009) 3559–3566.